Hypertension Research (2018) 41:809–816
https://doi.org/10.1038/s41440-018-0080-y

ARTICLE

Deletion of interferon-regulatory factor-1 results in cognitive impairment

Masaki Mogi[1] · Jun Iwanami[1] · Xiao-Li Wang[1] · Kana Tsukuda[1] · Harumi Kan-no[1] · Hui-Yu Bai[1] · Bao-Shuai Shan[1] · Akinori Higaki[1] · Li-Juan Min[1] · Masatsugu Horiuchi[1]

Received: 12 September 2017 / Revised: 19 February 2018 / Accepted: 25 March 2018 / Published online: 6 August 2018

Abstract

Interferon-regulatory factor (IRF)-1-dependent genes in neurons play a role in ischemic neuronal death; however, the roles of IRF-1 in dementia are not well investigated. Therefore, we assessed the effect of IRF-1 on cognitive function using a vascular cognitive impairment mouse model created by chronic cerebral hypoperfusion. Male 10-week-old C57BL/6 (wild-type; WT) and IRF-1-knockout (IRF-1KO) mice were used in this study. A chronic cerebral hypoperfusion mouse model was generated by bilateral common carotid artery stenosis (BCAS) treatment. After 6 weeks of BCAS, the mice were subjected to the Morris water maze test five times a day for 5 days. In the Morris water maze task, escape latency was significantly prolonged in sham-operated IRF-1KO mice compared with sham-operated WT mice. However, BCAS treatment cancelled such difference in spatial learning between WT and IRF-1KO mice. BCAS treatment decreased CBF, but no significant difference was observed between the two strains after BCAS. Sham-operated IRF-1KO mice showed a decrease in mRNA expression of caspase-1 and an increase in IRF-2 expression in the hippocampus. Expression of angiotensin II type 2 (AT_2) receptor, which induces better cognitive function, is regulated by IRF-1; however, no obvious difference in AT_2 receptor expression was observed between the two strains even after BCAS. These results suggest that IRF-1 has a protective effect on cognitive decline in a normal condition; however, there was no obvious effect on cognition after chronic cerebral hypoperfusion treatment.

Introduction

Vascular cognitive impairment is the second most common type of dementia and is associated with vascular risk factors such as hypertension, diabetes, and hyperlipidemia [1]. Reduced cerebral blood flow (CBF) owing to vascular dysfunction leads to hypoxia and ischemia, which initiates an inflammatory response with induction of proteases and free radicals and results in neuroinflammation [2]. In patients with vascular cognitive impairment, contrast-enhanced magnetic resonance imaging reveals regions of increased permeability within white matter hyperintensities with disruption of the blood–brain barrier (BBB) [3]. Therefore, neuroinflammation plays an important role in the progression of vascular cognitive impairment.

Interferon-regulatory factor-1 (IRF-1) in the brain has mainly been investigated in neuroinflammation such as encephalomyelitis [4–7]. In stroke, IRF-1 level is increased [8] and IRF-1KO mice showed reduced stroke size [9]. IRF-1 is essential for the induction of inducible nitric oxide synthase (iNOS) in macrophages [10, 11]. Sharma et al. [12] reported the protective effect of an iNOS inhibitor on vascular cognitive impairment induced by hypertension. These results suggest that IRF-1 regulates neuroinflammation and enhances the severity of brain injury partly via iNOS induction. On the other hand, our recent reports have indicated that stimulation of the angiotensin II type 2 (AT_2) receptor prevents cognitive decline [13] and IRF-1 induces AT_2 receptor expression [14–17], indicating that IRF-1 has a beneficial effect on cognitive decline via

Electronic supplementary material The online version of this article (https://doi.org/10.1038/s41440-018-0080-y) contains supplementary material, which is available to authorized users.

✉ Masaki Mogi
mmogi@m.ehime-u.ac.jp

[1] Department of Molecular Cardiovascular Biology and Pharmacology, Ehime University, Graduate School of Medicine, Matsuyama, Japan

AT_2 receptor signaling. However, the effect of IRF-1 on vascular injury-induced cognitive impairment has not been investigated. Bilateral carotid artery stenosis (BCAS) is a model for subcortical ischemic vascular cognitive impairment [18, 19], Therefore, we hypothesized that IRF-1 plays a role in BCAS-induced vascular cognitive impairment. To clarify this hypothesis, we employed IRF-1-deficient mice and assessed cognitive function with and without BCAS, focusing on neuroinflammation.

Methods

This study was performed in compliance with the National Institutes of Health guidelines for the use of experimental animals and under protocols reviewed and approved by the Animal Studies Committee of Ehime University.

Animals

The study procedure is shown in Fig. 1. Adult male C57BL/6 mice (Clea Japan Inc., Tokyo, Japan) as wild-type (WT) mice and IRF-1 knockout mice (IRF-1KO mice; based on C57BL/6 J strain) [20] (23–25 g; 10 weeks old) were used. Mice were housed in a room in which lighting was controlled (12 h on, 12 h off), and temperature was kept at 25 °C. They were given a standard diet (MF, Oriental Yeast, Tokyo, Japan) and water ad libitum. BCAS was induced by a microcoil technique as described previously [21]. We used a microcoil with inner diameter of 0.18 mm and total length of 2.5 mm (Sawane Spring Co., Hamamatsu, Japan). Mice were anesthetized with i.p. 65 mg/kg nembutal in saline. A midline incision was made in the neck, and the bilateral common carotid arteries were isolated. A silk suture was placed around the right common carotid artery (CCA). Then, the CCA was gently lifted by a suture and placed between the loops of the microcoil. The microcoil was twined around the CCA by rotating it. After that, another microcoil was twined around the left CCA in the same way. Sham operation was performed till isolation of the common carotid arteries. The microcoil's inner diameter of 0.18 mm resulted in a stenosis of ~ 50%, because the outer diameter of the CCA was 0.35–0.40 mm under anesthesia. We checked the cerebral blood flow before and just after BCAS operation. Cerebral blood flow just after BCAS operation was decreased to 60–70%. Systolic blood pressure was measured in conscious mice by the tail-cuff method (MK-1030; Muromachi Co., Tokyo, Japan) 6 weeks after BCAS operation. There was no significant difference in systolic blood pressure of WT and IRF-1KO mice with or without BCAS surgery (data not shown).

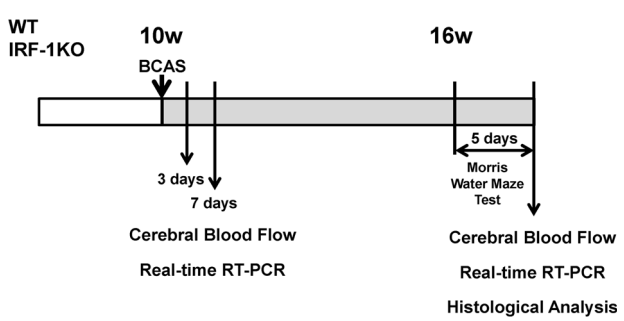

Fig. 1 Study procedure of this study. BCAS, bilateral common carotid artery stenosis

Morris water maze test

The Morris water maze task was performed in mice 6 weeks after the BCAS operation as previously described [22]. A white circular tank (120 cm diameter) was filled with water (23 ± 2 °C). A transparent platform (a 6 cm × 6 cm acrylic board) was placed 1.5 cm below the surface of the water. Four objects in the corners of the pool helped mice to know their position. After they were placed on the platform for 10 sec, they were put into the water. After reaching the platform, they were returned to their cages. If they did not reach the platform within 120 sec, they were placed on it, kept there for 10 sec, and returned to their cages. Mice were trained five times a day at 20-min intervals for 5 consecutive days. In each trial, mice were given 120 sec to find the platform. Swimming was video-tracked (Any-Maze, Wood Dale, IL), and latency, path length, swim speed, and cumulative distance from the platform were recorded. Mean swim latency each day was evaluated and compared between groups. The area under the curve of days 1–5 was quantified using computer-imaging software (Densitograph; ATTO Corporation, Tokyo, Japan). All analyses were performed by an investigator blinded to the experimental conditions.

Measurement of CBF

CBF was measured by laser speckle flowmetry (Omegazone laser speckle blood flow imager; Omegawave, Tokyo, Japan), which obtains high-resolution 2D images in a matter of seconds as previously described [13]. CBF was measured at 3 days, 7 days, and 6 weeks after BCAS surgery. Mice were anesthetized with i.p. Nembutal (75 mg/kg), and a midline incision was made in the scalp. The skull was exposed and wet with saline. A 780-nm laser semiconductor laser illuminated the whole skull surface. Mean CBF on the skull surface was measured. Light intensity was accumulated in a charge-coupled device camera and transferred to a computer for analysis. Image pixels were analyzed to

Table 1 Primers used for qPCR

Gene	Accession #	Forward	Reverse
IFNα	NM_206975	5′-CCTTCTGCAATGACCTCAACACT-3′	5′-AGGGGAGGTGCCTGTATCTCT-3′
IFNβ	NM_010510	5′-AGAGTTACACTGCCTTTGCCATC-3′	5′-CTGTCTGCTGGTGGAGTTCATC-3′
IFNγ	NM_008337	5′-TTACTACCTTCTTCAGCAACAGCAA-3′	5′-CTGGTGGACCACTCGGATGAG-3′
IRF-1	NM_008390	5′-CAGAGGAAAGAGAGAAAGTCC-3′	5′-CACACGGTGACAGTGCTGG-3′
IRF-2	NM_008391	5′-GCGGTCCTGACTTCAGCTATA-3′	5′-CTTCTTGATGACACTGGCCGG-3′
TNF-α	NM_013693.3	5′-CGAGTGACAAGCCTGTAGCC-3′	5′-GGTGAGGAGCACGATGTCG-3′
MCP-1	NM_011333.3	5′-TTAACGCCCCACTCACCTGCTG-3′	5′-GCTTCTTTGGGACACCTGCTGC-3′
IL-6	NM_031168.1	5′-CCACTTCACAAGTCGGAGGCTTA-3′	5′-GCAAGTGCATCATCGTTGTTCATAC-3′
p22phox	NM_001301284 NM_007806.3	5′-TGGCTACTGCTGGACGTTTCAC-3′	5′-CTCCAGGAGACAGATGAGCACAC-3′
p40phox	NM_008677.2	5′-TTTGAGCAGCTTCCAGACGA-3′	5′-GGTGAAAGGGCTGTTCTTGC-3′
p47phox	NM_001286037.1 NM_010876.4	5′-GTCCCTGCATCCTATCTGGA-3′	5′-GGGACATCTCGTCCTCTTCA-3′
p67phox	NM_010877.4	5′-CAGACCCAAAACCCCAGAAA-3′	5′-AGGGTGAATCCGAAGCTCAA-3′
gp91phox	NM_007807.5	5′-TGGGATCACAGGAATTGTCA-3′	5′-CTTCCAAACTCTCCGCAGTC-3′
AT_1 receptor	NM_177322.3	5′ - AGTCGCACTCAAGCCTGTCT-3′	5′-ACTGGTCCTTTGGTCGTGAG-3′
AT_2 receptor	NM_007429	5′-CACTGGCAACTAAAAAGGTAAGA-3′	5′-CGGCTGCTGGTAATGTTTCTG-3′
BDNF	NM_007540	5′-AGGACAGCAAAGCCACAATGT-3′	5′-CCTTCATGCAACCGAAGTATG-3′
Caspase-1	NM_009807	5′-TGAAGAGGATTTCTTAACGGATGC-3′	5′-GTCTCCAAGACACATTATCTGGTG-3′
PTGS/COX2	NM_011198	5′-AAGACAGATCATAAGCGAGGACCT-3′	5′-CACCTCTCCACCAATGACCTGAT-3′
ANXA2	NM_007585	5′-GGATGGCTCAGTTATTGACTACGA-3′	5′-CGTCGGTTCCTTTCCTCTTCAC-3′
CCNB1	NM_172301	5′-GAGTGACGTAGACGCAGATGATG-3′	5′-AGGATAGCTCTCATGTTTCCAGTCA-3′
iNOS	NM_010927	5′-GTCACCTACCGCACCCGAG-3′	5′-GCCACTGACACTTCGCACAA-3′
GAPDH	NM_001289726.1 NM_008084.3	5v- ATGTAGGCCATGAGGTCCAC-3′	5′-TGCGACTTCAACAGCAACTC-3′

produce average perfusion values. All analyses were performed by an investigator blinded to the experimental conditions.

Real-time reverse transcription polymerase chain reaction (RT-PCR) method

Brain samples were obtained at 3 days, 7 days, and 6 weeks after BCAS surgery. Thus, some mice were killed without the Morris water maze test. Samples of the hippocampus were frozen in liquid nitrogen and stored at −80 °C until analysis. Total mRNA was extracted from brain samples after homogenization in Sepazol (Nacalai Tesque Inc., Kyoto, Japan). Quantitative real-time RT-PCR was performed with a SYBR green kit (MJ Research, Inc., Waltham, MA). PCR primers were as follows: IFNα, IFNβ, IFNγ, IRF-1, IRF-2, tumor nuclear factor (TNF)-α, monocyte chemotactic protein (MCP)-1, IL-6, $p22^{phox}$, $p40^{phox}$, $p47^{phox}$, $p67^{phox}$, $gp91^{phox}$, angiotensin II type 1 (AT_1) receptor, AT_2 receptor, brain-derived neurotropic factor (BDNF), caspase-1, prostaglandin-endoperoxide synthase (2PTGS2/COX2), annexin A2 (ANXA2), cyclin B1 (CCNB1), and iNOS. Primer sequences are shown in Table 1.

Histological analysis

Brain samples were fixed with 4% paraformaldehyde and stored as paraffin-embedded samples. To assess the histopathological changes after BCAS surgery, we prepared 5-μm-thick paraffin sections and stained them with hematoxylin–eosin after deparaffinization. Coronal slices were selected between 1.82 mm and 2.31 mm posterior to the bregma to observe the hippocampal area. Samples were examined with an upright microscope (Axioskop 2, Carl Zeiss, Oberkochen, Germany) at ×400 magnification. The center of the CA1 area and the innermost portion of the granular cell layer in the dentate gyrus were set as the observation range. Average cell number per field from two slices with a 200-μm interval was counted with computer-imaging software (Densitograph, ATTO, Tokyo, Japan).

Statistical analysis

All values are expressed as mean ± standard error of the mean in the text and figures. Analysis of variance was also performed for each result. If a statistically significant effect was found, post hoc analysis with Tukey–Kramer method

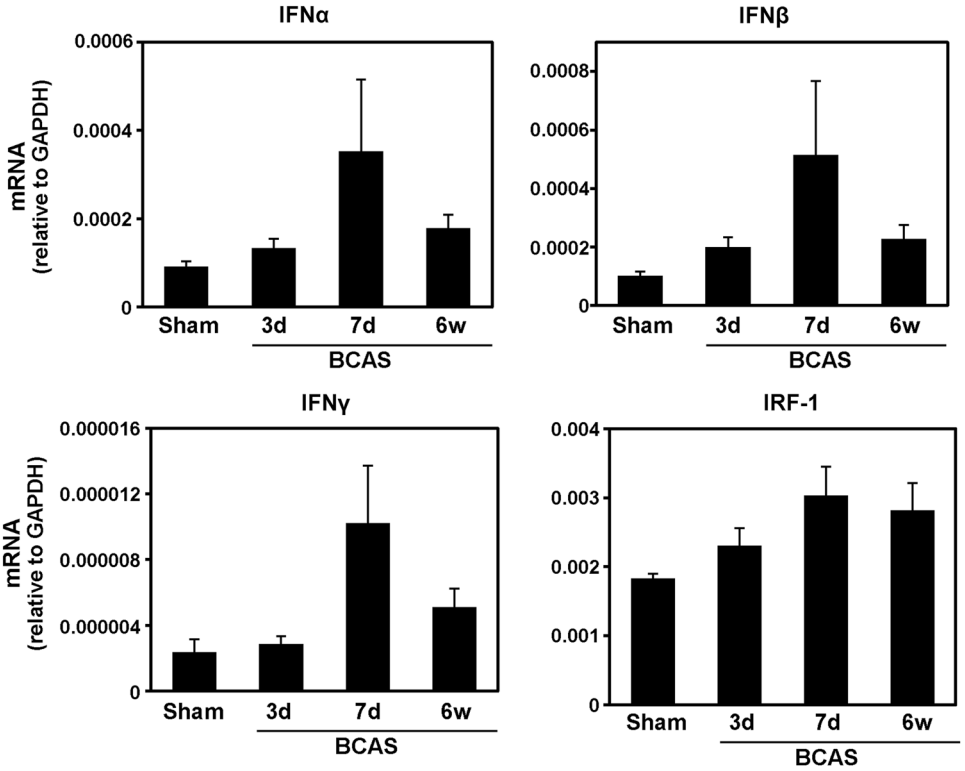

Fig. 2 Time course of IFNα, β, and γ and IRF-1 in hippocampus of WT mice after BCAS surgery. RT-PCR analysis was performed as described in "Methods". No significant difference was observed at each time. $N = 3$–4 for each group

was performed to detect the difference between the groups using Statcel ver.3 software. Data were evaluated by analysis of variance followed by post hoc analysis for multiple comparisons. A difference with $p < 0.05$ was considered significant.

Results

BCAS treatment enhanced levels of inflammatory cytokines after 7 days in WT mice

First, we analyzed the time-course mRNA expression of IFNα, β, and γ and IRF-1 in the hippocampus of WT mice after BCAS surgery to determine the peak of inflammatory cytokine expression (Fig. 2). Samples were prepared from sham, and 3 and 7 days and 6 weeks after BCAS surgery. Such expression increased after BCAS treatment and reached a peak after 7 days of BCAS.

IRF-1KO mice showed impaired cognitive function compared with WT mice, but BCAS treatment induced impairment of cognitive function in both WT and IRF-1KO mice

Sham-treated IRF-1KO mice showed prolonged escape latency on the third to fifth day of the trial compared with WT mice (Fig. 3). BCAS treatment prolonged mean escape latency in WT mice and also in IRF-1KO. However, there was no obvious difference in escape latency between the two strains with BCAS (Fig. 3). Swim speed was not different in each mouse group (Supplementary Fig. 1).

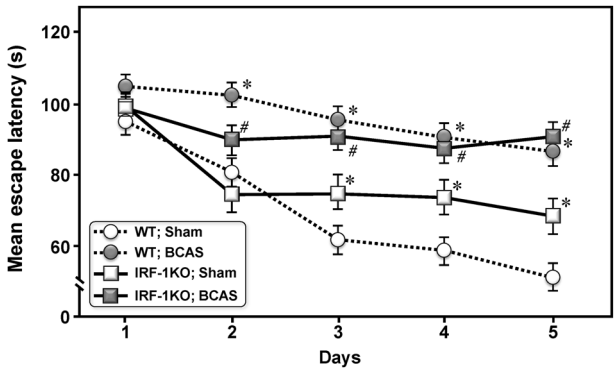

Fig. 3 Cognitive function in WT and IRF-1KO mice with and without BCAS. The Morris water maze test was performed according to "Methods". Mean escape latency on each training day is shown. #$p < 0.05$ vs. Sham (IRF-1KO), *$p < 0.05$ vs. Sham (WT). $n = 18$–23

Comparison of CBF in WT and IRF-1KO mice with and without BCAS

Figure 4 shows a comparison of CBF between WT and IRF-1KO mice. BCAS treatment decreased CBF in both strains, but no significant difference was observed between the two BCAS strains.

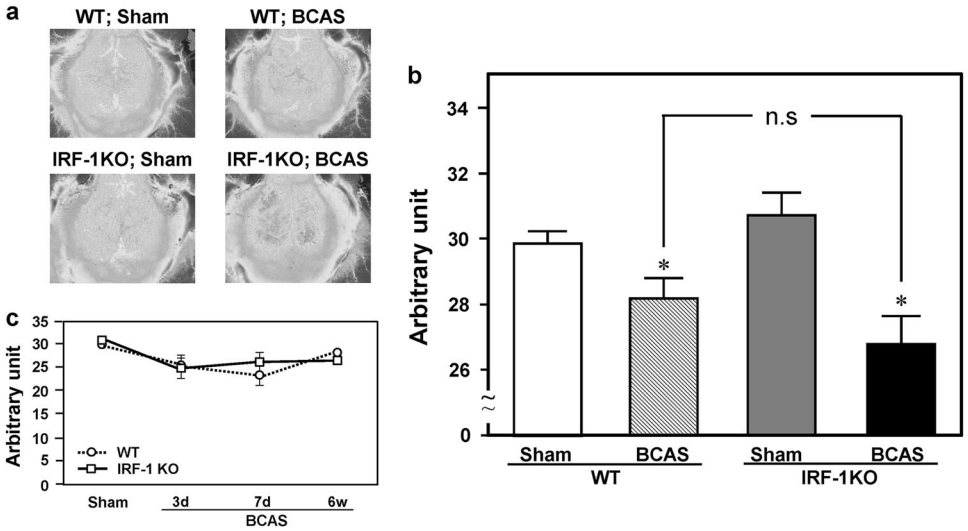

Fig. 4 CBF in WT and IRF-1KO mice with and without BCAS. **a** Representative photos of Doppler flowmetry. **b** Histogram analysis of CBF in each group. **c** Time-course analysis of CBF. Data are expressed as mean ± SEM. $*p < 0.05$ vs. Sham (WT). $n = 5–8$

Comparison of cell number in CA1 region between WT and IRF-1KO mice

To investigate whether there was a morphological change in the hippocampus of IRF-1KO mice, we counted the cell number in the CA1 region. No significant difference was observed between the two strains, even after BCAS surgery (Fig. 5).

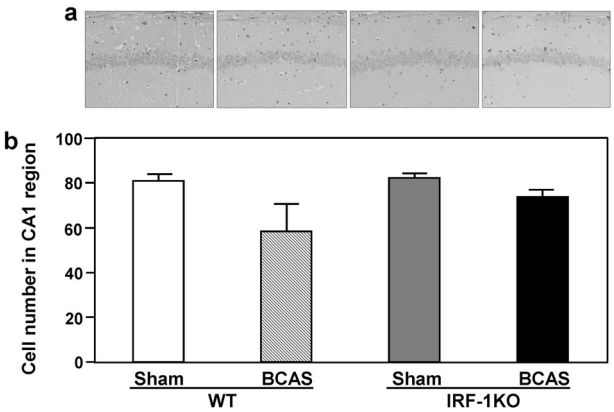

Fig. 5 Cell number in CA1 region in WT and IRF-1KO mice. **a** Representative photos of CA1 region. **b** Cell number in CA1 region in each group. $n = 4–5$

Comparison of mRNA expression in IRF-1KO mice compared with WT mice with and without BCAS

Next, we assessed mRNA expression in the hippocampus. Levels of inflammatory cytokines such as TNF-α, MCP-1, and IL-6 showed no significant change in sham-operated mice.

Interestingly, their expression increased earlier in IRF-1KO mice compared with WT mice after BCAS and reached a peak after 3 days of BCAS (Fig. 6a). IRF-1KO mice showed no increase in the levels of NADPH subunits after BCAS (Fig. 6b). BDNF level also increased earlier in IRF-1KO mice compared with WT mice after BCAS and reached a peak after 3 days of BCAS (Fig. 6c). On the other hand, no obvious difference in levels of angiotensin II receptors, especially in the AT_2 receptor, which was shown to induce better cognitive function in our previous report [13], was observed between the two strains even after BCAS (Fig. 6d).

Several isoforms exist in interferon-regulatory factors [23], and IRF-1 controls the transcription of various genes [24]. Next, we investigated the expression of several genes that are reported to be involved in cognitive function. Caspase-1 level was lower in IRF-1KO mice, even in non-treated mice (Fig. 7a). On the other hand, IRF-2 level was significantly higher in IRF-1KO mice than in non-treated mice. However, after BCAS, IRF-2 level was decreased, and there was no difference in its expression between WT and IRF-1-KO mice (Fig. 7b). In WT mice, a transient increase in IRF-1 regulated genes such as PTGS2, ANXA2, and CCNB1, but not in iNOS, was observed 7 days after BCAS treatment. However, these changes were not observed in IRF-1KO mice (Fig. 7c).

Discussion

The present study demonstrated that IRF-1KO mice showed impairment of cognitive function compared with WT mice in a normal condition, but no significant difference in cognitive function was observed between the two strains with BCAS, indicating that IRF-1 plays a key role in cognitive function in a normal condition.

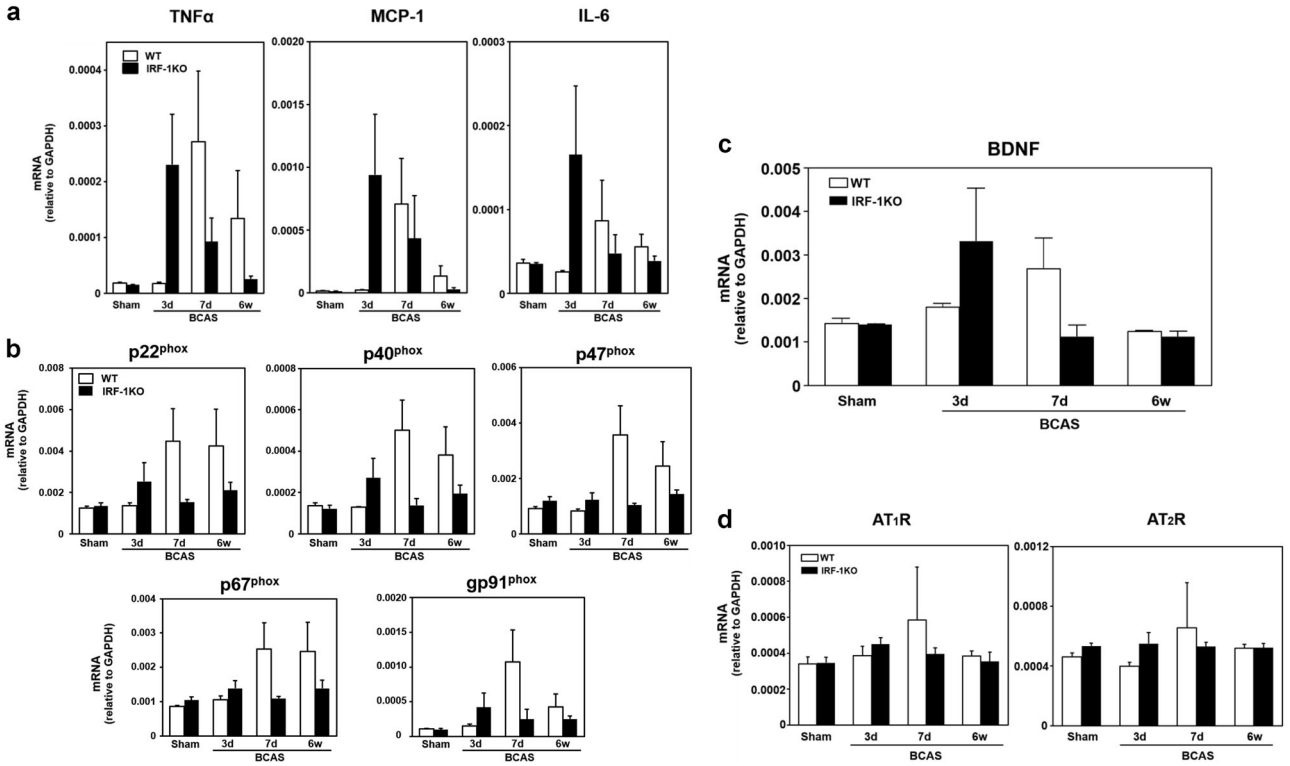

Fig. 6 Time course of mRNA expression in hippocampus of IRF-1KO mice and WT mice after BCAS. Time course of mRNA expression of inflammatory cytokines **a**, NADPH oxidase subunits (**b**), BDNF (**c**), and angiotensin II receptors (**d**)

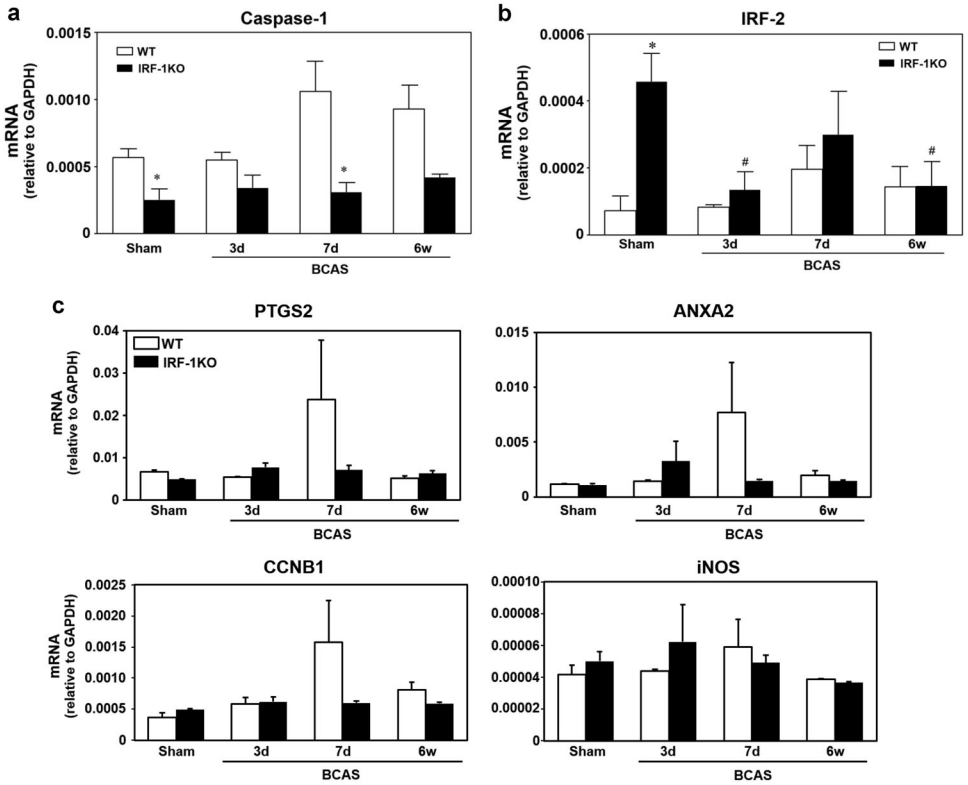

Fig. 7 IRF-1-related mRNA expression in hippocampus of IRF-1KO mice and WT mice after BCAS. Time course of mRNA expression of IRF-1 regulated genes such as caspase-1 **a**, IRF-2 **b**, and **c** PTGS2, ANXA2, CCNB1, and iNOS. Data are expressed as mean ± SEM. $*p < 0.05$ vs. Sham (WT), $\#p < 0.05$ vs. Sham (IRF-1KO). $n = 3$–4

Deletion of the IRF-1 gene induced impairment of learning ability in sham-operated mice. We investigated IRF-1-related genes, which are involved in cognitive function (Fig. 7), but no obvious difference in such expression including that of iNOS and the AT_2 receptor was observed in sham-operated mice. Interestingly, hippocampal IRF-2 expression was increased in IRF-1KO mice. IRF-2 suppresses the activity of IRF-1 by competing for binding sites within the promoters of IFN genes and potentially limiting the IFN response [25]. IRF-2 protects mice from lethal viral neuroinvasion via modulation of immune responses [26]. However, to our knowledge, the effect of IRF-2 in the brain on cognitive function in a healthy condition has not been investigated. Therefore, lack of the IRF-1 gene may compensatorily affect other IRF levels and IFN-induced functions. Studies of conditional gene modification mice may help to determine the detailed mechanism.

On the other hand, unknown IRF-1-regulatory factors may be involved in this mechanism. As shown in Fig. 3, there was a relatively flat learning curve in IRF-1KO mice from the second day of the trial. The learning process is based on two important aspects of long-term memory: creating a trace and consolidation of the received information. A flat learning curve indicates deficits of these processes [27]. For example, cell adhesion molecules (CAM) are involved in synaptic plasticity and memory consolidation [28]. There are several reports on the relation between CAM expression and IRF-1 [29, 30]. Therefore, IRF-1 may influence memory retention with modulation of CAM. Further investigation is necessary to determine the effect of IRF-1 on cognition involving CAM.

IRF-1KO with BCAS showed more impaired cognitive function compared with sham-treated IRF-1KO; however, there was no difference in vascular cognitive impairment between IRF-1KO and WT mice after BCAS. One of the reasons for the lack of difference in cognitive function after BCAS is considered to be the time lag in neuroinflammation observed in IRF-1KO mice. Hippocampus mRNA expression of inflammatory cytokines and BDNF reached a peak earlier in IRF-1KO mice compared with WT mice after BCAS. In other words, neuroinflammation was terminated faster in IRF-1KO mice compared with WT mice. Accumulation of inflammatory cells around damaged blood vessels is an important feature of the pathophysiology of Binswanger disease owing to hypoxic conditions [3]. Neuroinflammation promotes BBB disruption and leads to neurovascular deficits, resulting in neurodegeneration [31]. On the other hand, the damaged brain undergoes a transition from injury to repair [32]. Thus, earlier transition to a repair state may occur in IRF-1KO and prevent neuroinflammation-induced vascular cognitive impairment. Moreover, Wattananit et al. [33] recently demonstrated that blocking monocyte recruitment using an antibody during the first week after stroke abolished long-term behavioral recovery, indicating that appropriate regulation of inflammation contributes to long-term functional recovery after stroke. Although we did not assess monocyte recruitment in this model, the earlier reduction of neuroinflammation in IRF-1KO mice may contribute to progression of the brain repair pathway.

A limitation of this study is the small number of mRNA samples, which showed a wide range of the values, and the fact that only mRNA levels of expressed factors were measured in the brain, showing only gene expression and not actual protein expression. In addition, blood pressure levels should be assessed several times after BCAS. Moreover, a more comprehensive assessment of behavior and cognition including memory and cognitive flexibility in addition to learning would help to understand the role of IRF-1 in normal learning ability and vascular cognitive impairment. Further analysis to assess the detailed mechanism is necessary.

Conclusions

Our findings suggest that IRF-1 has a protective effect on cognitive decline in a normal condition; however, there was no obvious effect on cognition after chronic cerebral hypoperfusion treatment. The roles of IRF-1 in memory function should be further assessed beyond the relation between neuroinflammation and cognitive function.

Availability of data and materials

All data used for formulation of conclusions in the manuscript are presented in the main paper.

Author contributions MM performed experimental design, data interpretation, and manuscript preparation. JI performed experimental design, qPCR, data interpretation, and manuscript preparation. XLW performed experimental design, the Morris water maze test, BCAS surgery, CBF measurement, histological analysis, qPCR, data interpretation, and manuscript preparation. KT and HK performed qPCR. HYB, BSS, MK, TY, AH, and LJM performed data interpretation. MH performed experimental design, data interpretation, and drafting of the manuscript. All authors read and approved the final version of the manuscript.

Funding information This study was supported by JSPS KAKENHI [Grant Number 25293310 to M.H., 25462220 to M.M., 15K19974 to . I., and 26860567 to L.-J.M.], and research grants from pharmaceutical companies: Astellas Pharma Inc., Bayer Yakuhin, Ltd., Daiichi-Sankyo Pharmaceutical Co., Ltd., Nippon Boehringer Ingelheim Co., Ltd., Novartis Pharma K. K., Shionogi & Co., Ltd., and Takeda Pharmaceutical Co., Ltd. The funders had no role in the study design, data collection and analysis, decision to publish, or preparation of the manuscript.

Compliance with ethical standards

Conflict of interest The authors declare that they have no conflict of interest.

References

1. Duron E, Hanon O. Vascular risk factors, cognitive decline, and dementia. Vasc Health Risk Manag. 2008;4:363–81.
2. Rosenberg GA, Bjerke M, Wallin A. Multimodal markers of inflammation in the subcortical ischemic vascular disease type of vascular cognitive impairment. Stroke. 2014;45:1531–8.
3. Rosenberg GA. Inflammation and white matter damage in vascular cognitive impairment. Stroke. 2009;40:S20–3.
4. Tada Y, Ho A, Matsuyama T, Mak TW. Reduced incidence and severity of antigen-induced autoimmune diseases in mice lacking interferon regulatory factor-1. J Exp Med. 1997;185:231–8.
5. Ren Z, Wang Y, Liebenson D, Liggett T, Goswami R, Stefoski D, et al. IRF-1 signaling in central nervous system glial cells regulates inflammatory demyelination. J Neuroimmunol. 2011;233: 147–59.
6. Ren Z, Wang Y, Tao D, Liebenson D, Liggett T, Goswami R, et al. Overexpression of the dominant-negative form of interferon regulatory factor-1 in oligodendrocytes protects against experimental autoimmune encephalomyelitis. J Neurosci. 2011;31: 8329–41.
7. Ren Z, Wang Y, Tao D, Liebenson D, Liggett T, Goswami R, et al. Central nervous system expression of interferon regulatory factor-1 regulates experimental autoimmune encephalomyelitis. J Neuroimmune Pharmacol. 2010;5:260–5.
8. Paschen W, Gissel C, Althausen S, Doutheil J. Changes in interferon-regulatory factor-1 mRNA levels after transient ischemia in rat brain. Neuroreport. 1998;9:3147–51.
9. Iadecola C, Salkowski CA, Zhang F, Aber T, Nagayama M, Vogel SN, et al. The transcription factor interferon regulatory factor-1 is expressed after cerebral ischemia and contributes to ischemic brain injury. J Exp Med. 1999;189:719–27.
10. Martin E, Nathan C, Xie QW. Role of interferon regulatory factor-1 in induction of nitric oxide synthase. J Exp Med. 1994;180: 977–84.
11. Reis LF, Ruffner H, Stark G, Aguet M, Weissmann C. Mice devoid of interferon regulatory factor-1 (IRF-1) show normal expression of type I interferon genes. EMBO J. 1994;13: 4798–806.
12. Sharma B, Singh N. Pharmacological inhibition of inducible nitric oxide synthase (iNOS) and nicotinamide adenine dinucleotide phosphate (NADPH) oxidase, convalesce behavior and biochemistry of hypertension induced vascular dementia in rats. Pharmacol Biochem Behav. 2013;103:821–30.
13. Jing F, Mogi M, Sakata A, Iwanami J, Tsukuda K, Ohshima K, et al. Direct stimulation of angiotensin II type 2 receptor enhances spatial memory. J Cereb Blood Flow Metab. 2012;32:248–55.
14. Akishita M, Horiuchi M, Yamada H, Zhang L, Shirakami G, Tamura K, et al. Inflammation influences vascular remodeling through AT2 receptor expression and signaling. Physiol Genomics. 2000;2:13–20.
15. Horiuchi M, Hayashida W, Akishita M, Yamada S, Lehtonen JY, Tamura K, et al. Interferon-gamma induces AT(2) receptor expression in fibroblasts by JAK/STAT pathway and interferon regulatory factor-1. Circ Res. 2000;86:233–40.
16. Horiuchi M, Koike G, Yamada T, Mukoyama M, Nakajima M, Dzau VJ. The growth-dependent expression of angiotensin II type 2 receptor is regulated by transcription factors interferon regulatory factor-1 and -2. J Biol Chem. 1995;270:20225–30.
17. Horiuchi M, Yamada T, Hayashida W, Dzau VJ. Interferon regulatory factor-1 up-regulates angiotensin II type 2 receptor and induces apoptosis. J Biol Chem. 1997;272:11952–8.
18. Shibata M, Yamasaki N, Miyakawa T, Kalaria RN, Fujita Y, Ohtani R, et al. Selective impairment of working memory in a mouse model of chronic cerebral hypoperfusion. Stroke. 2007;38: 2826–32.
19. Shibata M, Ohtani R, Ihara M, Tomimoto H. White matter lesions and glial activation in a novel mouse model of chronic cerebral hypoperfusion. Stroke. 2004;35:2598–603.
20. Matsuyama T, Kimura T, Kitagawa M, Pfeffer K, Kawakami T, Watanabe N, et al. Targeted disruption of IRF-1 or IRF-2 results in abnormal type I IFN gene induction and aberrant lymphocyte development. Cell. 1993;75:83–97.
21. Iwanami J, Mogi M, Tsukuda K, Wang XL, Nakaoka H, Kan-no H, et al. Direct angiotensin II type 2 receptor stimulation by compound 21 prevents vascular dementia. J Am Soc Hypertens. 2015;9:250–6.
22. Sakata A, Mogi M, Iwanami J, Tsukuda K, Min LJ, Fujita T, et al. Sex-different effect of angiotensin II type 2 receptor on ischemic brain injury and cognitive function. Brain Res. 2009;1300: 14–23.
23. Lohoff M, Mak TW. Roles of interferon-regulatory factors in T-helper-cell differentiation. Nat Rev Immunol. 2005;5:125–35.
24. Chen FF, Jiang G, Xu K, Zheng JN. Function and mechanism by which interferon regulatory factor-1 inhibits oncogenesis. Oncol Lett. 2013;5:417–23.
25. Harada H, Fujita T, Miyamoto M, Kimura Y, Maruyama M, Furia A, et al. Structurally similar but functionally distinct factors, IRF-1 and IRF-2, bind to the same regulatory elements of IFN and IFN-inducible genes. Cell. 1989;58:729–39.
26. Li MM, Bozzacco L, Hoffmann HH, Breton G, Loschko J, Xiao JW, et al. Interferon regulatory factor 2 protects mice from lethal viral neuroinvasion. J Exp Med. 2016;213:2931–47.
27. Mitrovic SM, Dickov A, Vuckovic N, Mitrovic D, Budisa D. The effect of heroin on verbal memory. Psychiatr Danub. 2011;23: 53–9.
28. Wright JW, Kramar EA, Meighan SE, Harding JW. Extracellular matrix molecules, long-term potentiation, memory consolidation and the brain angiotensin system. Peptides. 2002; 23:221–46.
29. Nizamutdinova IT, Kim YM, Lee JH, Chang KC, Kim HJ. MKP-7, a negative regulator of JNK, regulates VCAM-1 expression through IRF-1. Cell Signal. 2012;24:866–72.
30. Neish AS, Read MA, Thanos D, Pine R, Maniatis T, Collins T. Endothelial interferon regulatory factor 1 cooperates with NF-kappa B as a transcriptional activator of vascular cell adhesion molecule 1. Mol Cell Biol. 1995;15:2558–69.
31. Zlokovic BV. Neurovascular pathways to neurodegeneration in Alzheimer's disease and other disorders. Nat Rev Neurosci. 2011;12:723–38.
32. Lo EH. A new penumbra: transitioning from injury into repair after stroke. Nat Med. 2008;14:497–500.
33. Wattananit S, Tornero D, Graubardt N, Memanishvili T, Monni E, Tatarishvili J, et al. Monocyte-derived macrophages contribute to spontaneous long-term functional recovery after stroke in mice. J Neurosci. 2016;36:4182–95.